Chapter 5

Analysis of Quantization Effects in Adaptive Base Station Antennas for Cellular Systems

5.1 Introduction

Over the last few years the telecommunications industry has grown beyond all expectations. An explosive increase is predicted in the number of subscribers in mobile telephone networks over the world. This enormous increase in the number of users introduces an extraordinary technological challenge: to provide wireless networks with spectral efficiencies to cope with these demands.

Adaptive antennas are by many expected to be a key component in the wireless networks of the future. The spatial signal processing provided by an adaptive array antenna at the base station site gives the desired enhancement of spectral efficiency [25] through the novel Spatial Division Multiple Access (SDMA) scheme complementing Frequency/Time Division Multiple Access (F/TDMA) or Code Division Multiple Access (CDMA). The spatial processing is in fact a filter that suppresses transmission to, and reception from, undesired directions. An important question is which factors limit the antennas ability to suppress unwanted signals. Studies have been done on temperature drift in receivers, on linearity requirements [26], on inaccuracies in weights [27], [28] and on the required precision when performing weight calculations [29]. Also the array configuration and array errors decrease the performance as investigated by Steyskal in [24], and Winters and co-workers in [30]. Different algorithms are proposed to be implemented in future adaptive

base station antennas and their benefits and drawbacks are under investigation. These algorithms also introduce errors, many of which are algorithm specific, for example the estimation of the covariance matrix in the direct methods or the estimation of direction of arrivals in indirect approaches [31]. In this chapter, some factors that degrade the adaptive antenna performance are examined and comparisons are made with measured results.

In different projects around the world adaptive antennas are built to give *proof-of-concept* trials, to examine the impact of adaptive antennas in wireless networks and to give knowledge on actual implementation techniques [10], [11]. The spatial filtering by the adaptive antenna can be implemented completely digitally in a signal processor. It can also be implemented with a hybrid digital-analog design, using an analog hardware implementation of the weights (on the RF) that are calculated in a digital signal processor. The hybrid digital-analog design dates back to the traditional phased-array approach. A drawback with the hybrid design is the inflexibility when adding a SDMA channel, which needs a new set of hardware weights. Also the number of bits used when setting the analog weights are a limiting factor for the antenna performance.

The complexity in the fully digital design lies in the requirement for high performing analog to digital and digital to analog converters necessary for the digital beamformer and in the required computation speed of the digital signal processor. High demands are put on the dynamic range and sample rate, not to mention the amount of data that has to be reduced prior to processing.

We shall discuss an adaptive antenna built for the DCS-1800 (Digital Communication System) system, also presented in Chapter 4. It works in the receiving mode only and uses the hybrid digital-analog weighting technique. This technique was chosen because it provided the possibility to connect the beamformer output to an existing base station receiver for downconversion, equalization and detection. DCS-1800 frames can therefore be used in the transmission to emulate a realistic communication without having to re-design a complete system for detection and equalization. The use of hybrid analog-digital weights provides an opportunity to examine the impact of phase errors and amplitude errors in the beamforming weights, by treating them as an equivalent quantization noise.

In this chapter the impact of quantization of weights in hybrid analog-digital beamforming is investigated using the output Signal to Interferer plus Noise Ratio (SINR) as a figure of merit. We extend the derivations of

Compton [20] by introducing quantization of the hardware weights. The magnitude is quantized in logarithmic steps as opposed to the linear quantization examined by Davis and Sher in [28]. The Digital Beamformer (DBF) is then discussed in a comparative manner. Also the Bit Error Rate (BER) is used as an evaluation parameter. The theoretical results are used to interpret the performance of the adaptive antenna from measurements in the laboratory and from field trials. For completeness, we now present the basic principles of array antennas.

5.2 Principles of Array Antennas

In this section, an expression is derived for the SINR of the adaptive antenna output, assuming narrowband signals. The approximation error introduced hereby is discussed. Further more, the relation between SINR performance of the adaptive antenna and the spatial correlation coefficient is examined. Line of sight propagation between mobile and base, without multipath propagation is assumed throughout the discussion. The theoretical results will then be utilized in Section 5.3

5.2.1 Derivation of SINR

Consider two plane waves impinging on an array antenna of arbitrary structure and element type. The plane waves originate from two uncorrelated signal sources denoted the desired and interfering signal source. The aim of the signal processing in the receiver is to enhance the desired signal and simultaneously suppress the interferer. In this *theoretical* discussion, the antenna signals of the array corresponding to the desired signal are collected in a vector $\mathbf{x}_d$ given by

$$\mathbf{x}_d = A_d e^{j(\omega_0 t + \psi_d)} \mathbf{u}_d \tag{5.1}$$

where

$$A_d e^{j\psi_d} \tag{5.2}$$

is the complex base band signal from the desired source at the array with envelope A_d and phase ψ_d, the variable ω_0 is the carrier frequency and $\mathbf{u}_d$ the array response vector given by

$$\mathbf{u}_d = \begin{bmatrix} f_1(\theta_d, \phi_d, p_d)e^{-j\phi_{d1}} \\ f_2(\theta_d, \phi_d, p_d)e^{-j\phi_{d2}} \\ \mathbf{M} \\ f_N(\theta_d, \phi_d, p_d)e^{-j\phi_{dN}} \end{bmatrix}. \tag{5.3}$$

Here f_j is the complex radiation pattern (magnitude- and phase pattern) of the jth antenna element as a function of the desired signal elevation angle θ_d, the azimuth angle ϕ_d and the polarization p_d. The angles are measured relative to a fixed Cartesian coordinate system. The angle ϕ_{dj} is the phase shift of the jth antenna channel relative to the coordinate origin, introduced by the array structure, i.e.

$$\phi_{dj} = \mathbf{k}_d \cdot \mathbf{r}_j \tag{5.4}$$

where $\mathbf{k}_d$ is the normalized propagation vector of the desired signal and $\mathbf{r}_j$ is the normalized radius vector of the jth element. The interfering signal source will result in an input vector at the array of similar structure as that of (5.1), namely

$$\mathbf{x}_i = A_i e^{j(\omega_0 t + \psi_i)} \mathbf{u}_i \tag{5.5}$$

where A_i denotes the amplitude and ψ_i the phase.. Also assume spatially and temporally uncorrelated noise with power σ^2 in each antenna channel. This gives a total input vector

$$\mathbf{x} = \mathbf{x}_d + \mathbf{x}_i + \mathbf{x}_n \tag{5.6}$$

where $\mathbf{x}_n$ is the noise vector.

The elements of the input vector $\mathbf{x}$ are multiplied by complex-valued weights, collected in a weight vector $\mathbf{w}$, to form the output of the adaptive antenna y, i.e. $y = \mathbf{w}^T\mathbf{x}$. The weights are chosen to minimize the mean square error of the difference between the output y and a reference signal r, giving the criterion

$$\mathbf{w} = \min_{\mathbf{w}} E(|y - r|^2) = \min_{\mathbf{w}} E(|\mathbf{w}^T\mathbf{x} - r|^2) \tag{5.7}$$

where E is the expectation and ^{T} the matrix transpose. The reference signal r is assumed to be coherent with the desired signal $A_d e^{j(\omega_0 t + \psi_d)}$ and to be given by

$$r(t) = R e^{j(\omega_0 t + \psi_d)} \tag{5.8}$$

where R is the magnitude. The weight vector $\mathbf{w}$ can be calculated by solving a system of linear equations, see e.g. [11], given by

$$\mathbf{\Phi}\mathbf{w} = \mathbf{s} \tag{5.9}$$

where $\mathbf{\Phi}$ is the covariance matrix of the input $\mathbf{x}$ defined as

$$\mathbf{\Phi} = E\left\{\mathbf{x}^*\mathbf{x}^T\right\} \tag{5.10}$$

with * denoting complex conjugate. The vector $\mathbf{s}$ is the cross correlation between the input $\mathbf{x}$ and the reference signal r, i.e.

$$\mathbf{s} = E\left\{\mathbf{x}^* r\right\}. \tag{5.11}$$

The expressions for $\mathbf{x}$ and r above result in the following covariance matrix and cross-correlation vector:

$$\mathbf{\Phi} = \sigma^2\mathbf{I} + A_d^2\mathbf{u}_d^*\mathbf{u}_d^T + A_i^2\mathbf{u}_i^*\mathbf{u}_i^T \tag{5.12}$$

$$\mathbf{s} = RA_d\mathbf{u}_d^*. \tag{5.13}$$

An *explicit* expression for the weight vector

$$\mathbf{w} = \mathbf{\Phi}^{-1}\mathbf{s} \tag{5.14}$$

can be obtained by applying the matrix inversion lemma twice to the covariance matrix of (5.12), see Compton [20].

The mean power of the desired signal, the interferer and the noise at the output of the adaptive antenna are given by

$$P_d = \frac{1}{2} E\left\{ \left| \mathbf{w}^T \mathbf{x}_d \right|^2 \right\}$$

$$P_i = \frac{1}{2} E\left\{ \left| \mathbf{w}^T \mathbf{x}_i \right|^2 \right\} \tag{5.15}$$

$$P_n = \frac{1}{2} E\left\{ \left| \mathbf{w}^T \mathbf{x}_n \right|^2 \right\}$$

where the factor 1/2 originates from the squared effective value of the carriers. Using the expression of [20, p. 144] the SINR of the adaptive antenna output can be expressed as

$$SINR = \frac{P_d}{P_i + P_n} = \xi_d \left[\mathbf{u}_d^T \mathbf{u}_d^* - \frac{\left| \mathbf{u}_d^T \mathbf{u}_i^* \right|^2}{\xi_i^{-1} + \mathbf{u}_i^T \mathbf{u}_i^*} \right] \tag{5.16}$$

where

$$\xi_d = \frac{A_d^2}{\sigma^2} \tag{5.17}$$

is the desired-signal-to-noise-ratio per antenna channel and

$$\xi_i = \frac{A_i^2}{\sigma^2} \tag{5.18}$$

the interfering-signal-to-noise-ratio per channel.

The expression (5.16) has been calculated under the assumption that the desired signal and the interferer, given by (5.1) and (5.5), respectively, are of zero bandwidth. However, the reasoning can be generalized straightforwardly to the non-zero-bandwidth case with digitally modulated pulse shaped signals, the only difference being a new expression for the mean symbol power, provided that the relative bandwidth (ratio of bandwidth and carrier frequency) of the signal is sufficiently small.

A non-zero bandwidth plane wave impinging on a *uniform linear array* (isotropic elements with an inter-element spacing of $\lambda/2$) can be

approximated with a sinusoid and be treated in the framework above if the following criterion holds [20]:

$$\text{sinc}\left\{\frac{1}{2} B(N-1)\phi\right\} \approx 1 \tag{5.19}$$

where B is the relative bandwidth, N the number of antenna elements and ϕ is the interelement phase shift ranging from $-\pi$ to π. Sinc(x) denotes the sinx/x function. Most modern FDMA and TDMA systems will fulfill the requirements (5.19).

Example:
For the DCS-1800 system, we have $B \approx 10^{-4}$, $\phi_{max}=\pi$ (corresponding to an incoming angle of 90° relative to the normal of the array) and N=8, giving sinc{B(N-1)ϕ/2}=0.9999998. Similar criteria can be stated for other element configurations.

5.2.2 Spatial Correlation and Its Impact on Adaptive Array Performance

Revisiting (5.16) one observes that the SINR is affected by the term $\mathbf{u}_d^T \mathbf{u}_i^*$ which can be related to the important parameter denoted spatial correlation between the desired and interfering signal. In fact the spatial correlation α is the term in (5.16) after normalization:

$$\alpha = \frac{\left|\mathbf{u}_d^T \mathbf{u}_i^*\right|}{\sqrt{\mathbf{u}_d^T \mathbf{u}_d^*} \sqrt{\mathbf{u}_i^T \mathbf{u}_i^*}} = \cos\varphi \tag{5.20}$$

The parameter α is dependent on the antenna element position, the radiation patterns and the polarization properties as well as on the impinging signal directions. However it is not dependent on the signal powers of the interferer and the desired signal. It is convenient to summarize all this information into the single parameter α and investigate its impact on the adaptive antenna performance, utilizing (5.16). The spatial correlation coefficient can be generalized to the case when numerous interferers are present. It can then be represented as the

generalized angle φ between the desired signal vector and the hyperplane spanned by the interfering signal vectors in an N dimensional space, where N is the number of antenna elements [30].

When the two signals are spatially uncorrelated, i.e. when $\alpha \rightarrow 0$, the SINR on the antenna output in (5.16) attains the Signal to Noise Ratio (SNR) on the antenna input. Thus, the interferer is perfectly suppressed. Conversely, with a high spatial correlation the SINR in (5.16) approaches the limit

$$A_d{}^2\mathbf{u}_d{}^T\mathbf{u}_d{}^* / (\sigma^2 + A_i{}^2\mathbf{u}_i{}^T\mathbf{u}_i{}^*) \tag{5.21}$$

which is recognized as the SINR when no interferer suppression is present, i.e. the SINR on the antenna input. When the desired and interfering signals are located with a small angular separation, seen from the base station site, the spatial correlation α is high and the two signals cannot be separated. From this reasoning we conclude that there must be a critical angle separation between the desired and the interfering mobile where the SINR becomes unacceptable for correct reception of the desired signal. This critical angle is dependent on the power in the desired and interfering signal and is an important figure of merit for the antenna array when utilizing adaptive antennas in base stations. It determines when a handover within a cell in a full reuse (cluster size of one cell) SDMA system is necessary.

To increase the SINR of the adaptive antenna output, a reduction in the spatial correlation coefficient α is crucial. Effort should be put into designing the array to reduce this coefficient. However, directions of arrival of the signals are not known *a priori* so optimization of the array is a difficult task. Some general rules for reducing the spatial correlation coefficient is presented in [30]. One approach is to use high angular resolution arrays with irregularly placed elements.

5.3 Derivation of Weight Error Variance

Errors will be introduced in the weights of (5.14) since the expectations in (5.12) and (5.13) must be approximated based on a limited number of data points. If the weighting is done by hardware, errors due to the practical implementation of the hardware weights cannot be completely eliminated. Another source of error is the quantization of the hardware weights.

In this section, we shall study the error introduced by the weight quantization. An expression is derived for the variance of the weight error, assuming uniform distribution of phase errors and amplitude errors. The results are used in later sections to calculate the SINR using analog weighting .

The analog weights introduce errors due to the imprecise settings of phase shifters and attenuators. These errors affect the performance and interferer suppression capabilities of the adaptive antenna. Nitzberg [29] showed how the errors in adaptive weights affected the output power. Davis and Sher [28] derived the statistical properties of the weight errors for Inphase-Quadrature (I-Q), Phase-Phase (PP) and linear Phase-Amplitude (lin-PA) weighting, where in lin-PA the amplitude steps are equally spaced, resulting in an amplitude independent absolute amplitude error.

In this section, error statistics for logarithmic Phase-Amplitude (log-PA) weights are derived, following the *notation* of [28]. The motivation is that the theoretical results presented in this work are verified in Section 5.7 using an adaptive antenna with this kind of weighting. In log-PA, the amplitude steps are logarithmic (in dB steps), giving an amplitude independent relative error in the weight as opposed to lin-PA, where the relative error is amplitude dependent. A single weight can be written in polar notation as

$$w = Ae^{j\theta} \tag{5.22}$$

where A is the amplitude and θ is the phase. For the distribution of allowable weights in the complex plane, see Figure 5.1. Note that in log-PA small weight amplitudes provide accurate setting as opposed to the lin-PA where the weights are evenly distributed in the complex plane. As a consequence, the error variance due to quantization errors will increase with weight amplitude when log-PA is used.
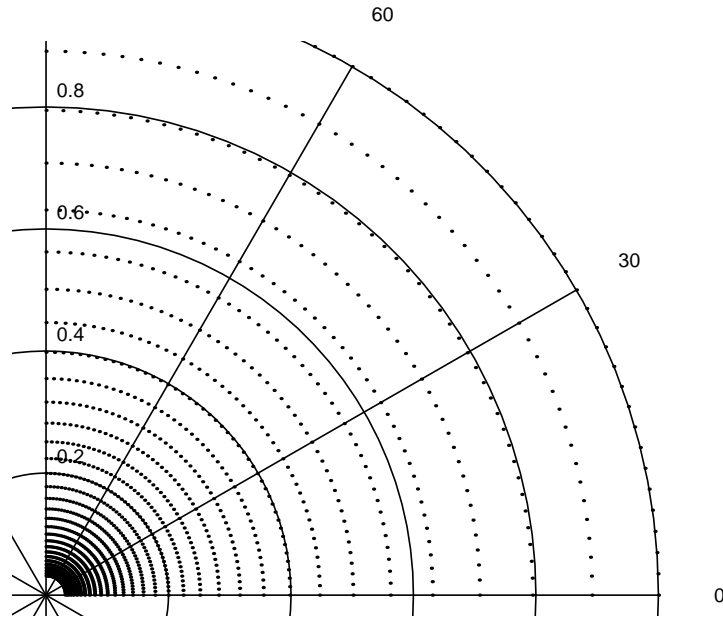
(a)
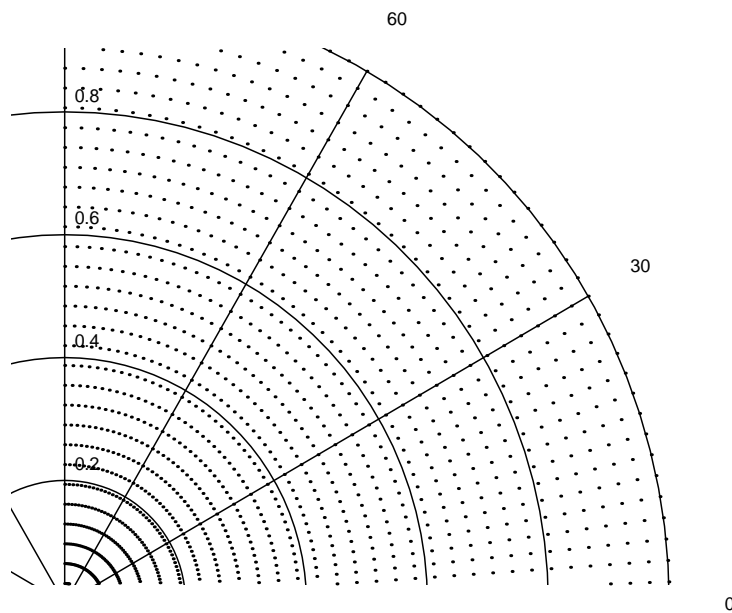
(b)

Fig. 5.1 Distribution of allowed weight vector in one quadrant of the complex plane for log-PA (a) and lin-PA (b).

Assume that $\theta \in [0,2\pi[$ and $A \in [0,1]$. Now, assume that the amplitude error dA and the phase error $d\theta$ due to implementation and quantization are independent random variables. Assume the amplitude error dA in log-PA to be uniformly distributed in the interval $[-\varepsilon_A A, \varepsilon_A A]$ due to the constant relative error $dA/A = \varepsilon_A$. Also, assume that the phase error $d\theta$ is uniformly distributed in $[-\varepsilon_\theta, \varepsilon_\theta]$. We will now derive an expression for the *squared*

magnitude error of the weight, $\Delta^2 = |\hat{w} - w|^2$, where $\hat{w}$ is the weight we have to use due to the weight quantization and w is the weight we want to use. By differentiating (5.22) with respect to A and θ and collecting terms, see [28], we obtain

$$|\Delta|^2 = (dA)^2 + A^2(d\theta)^2. \tag{5.23}$$

To simplify the notation, let $x = dA$, $y = Ad\theta$ and thus $z = x^2 + y^2$. Now, since $z = |\Delta|^2 \geq 0$, its Cumulative Distribution Function (CDF) $F_Z(z)$ equals the total probability mass in the circle of radius $\sqrt{z}$ for $z \geq 0$. The derivation of $F_Z(z)$ is separable in the two cases, the relative amplitude error ε_A is larger than the phase error ε_θ or vice versa. The calculations are similar and only the former will be outlined here. The calculation can be divided into four parts (I-IV), see Figure 5.2.
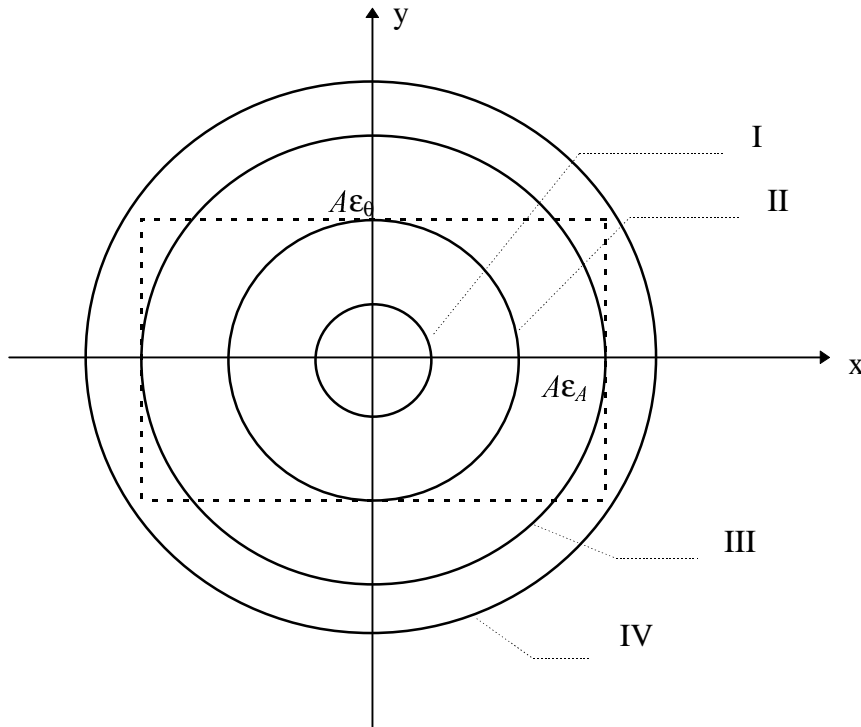
Fig. 5.2. Quantization of error distribution diagram. I: Circle inside rectangle, II: Circle limited at y-axis, III: Circle limited at x and y axis, III: Circle outside rectangle.

The two-dimensional probability density is $f_{XY}(x,y) = 1/(4\varepsilon_A\varepsilon_\theta A^2)$ for $|x| \leq A\varepsilon_A$ and $|y| \leq A\varepsilon_\theta$. With use of this the CDF for z can be calculated in the different regions above as

$$
F_Z(z) = \begin{cases}
\dfrac{\pi}{4\varepsilon_A\varepsilon_\theta A^2}\, z & 0 \le z \le \varepsilon_\theta^2 A^2 \\[2ex]
\dfrac{z}{2\varepsilon_A\varepsilon_\theta A^2}\left\{\arcsin\left(\dfrac{\varepsilon_\theta A}{\sqrt{z}}\right) + \dfrac{\varepsilon_\theta A}{z}\sqrt{z-\varepsilon_\theta^2 A^2}\right\} & \varepsilon_\theta^2 A^2 \le z \le \varepsilon_A^2 A^2 \\[2ex]
\dfrac{z}{2\varepsilon_A\varepsilon_\theta A^2}\left\{\arcsin\left(\dfrac{\varepsilon_\theta A}{\sqrt{z}}\right) + \dfrac{\varepsilon_\theta A}{z}\sqrt{z-\varepsilon_\theta^2 A^2} - \right. & \\
\left. -\arccos\left(\dfrac{\varepsilon_A A}{\sqrt{z}}\right) + \dfrac{\varepsilon_A A}{z}\sqrt{z-\varepsilon_A^2 A^2}\right\} & \varepsilon_A^2 A^2 \le z \le (\varepsilon_A^2+\varepsilon_\theta^2)A^2 \\[2ex]
1 & z \ge (\varepsilon_A^2+\varepsilon_\theta^2)A^2
\end{cases}
$$

$$(5.24)$$

Taking the derivative of the CDF with respect to z the Probability Density Function (PDF) is obtained. Using this PDF, the expected value of the squared magnitude error (z) can be calculated as

$$
E\left(\left|\Delta\right|^2\right) = \frac{1}{3}\,A^2\left(\varepsilon_A^2 + \varepsilon_\theta^2\right). \tag{5.25}
$$

This error is a function of the weight magnitude (A). From (5.25), an upper bound of the weight quantization error variance can be calculated.
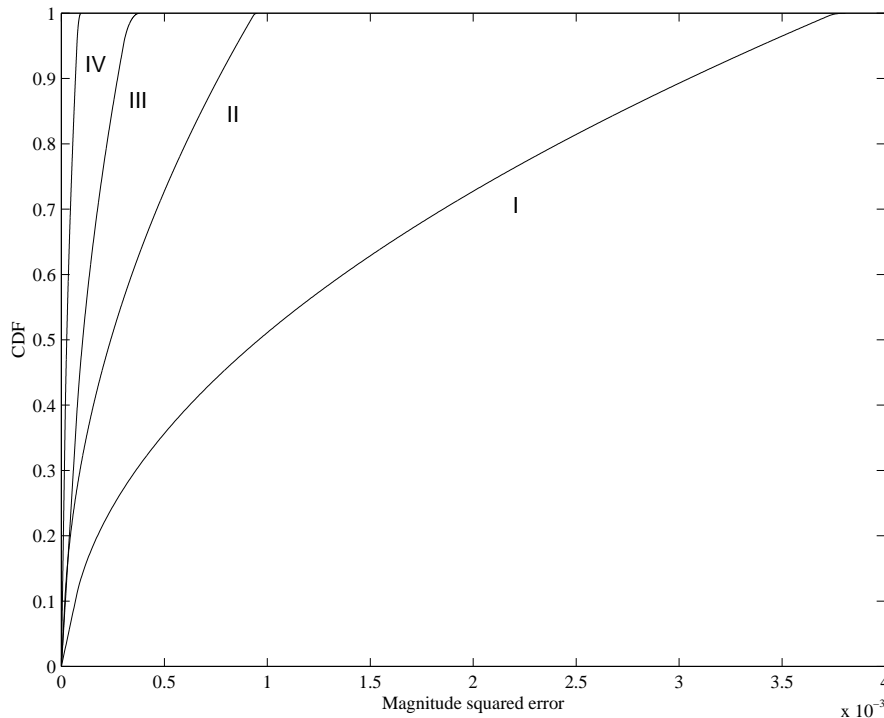
Fig. 5.3. The magnitude squared error CDF for different weight amplitudes (A) and amplitude errors (ε_A). The phase error $\varepsilon_\theta=0.5°$. I: $A=1$, $\varepsilon_A=7\varepsilon_\theta$, II: $A=1$, $\varepsilon_A=2\varepsilon_\theta$, III: $A=0.5$, $\varepsilon_A=7\varepsilon_\theta$, IV: $A=0.5$, $\varepsilon_A=2\varepsilon_\theta$.

In Figure 5.3 the CDF for some cases are plotted. We see that the slope of the CDF is strongly amplitude dependent, due to the way the weight amplitude impacts on both amplitude errors and phase errors. The results differs markedly from that for lin-PA weighting where the weight amplitude only affects the phase error, see Figure 14 in [28]. When there is imbalance in phase and amplitude accuracy as in curve I and III in Figure 5.3, a change in weight amplitude affects the CDF slope more than the small imbalance case in curve II and IV. This means that *the phase error* ε_θ *and amplitude error* ε_A *should be balanced*, i.e. nearly equal, to reduce the effect of the weight amplitude on the magnitude squared error.

5.4 Analog Beamforming

Adaptive antennas where the weights are calculated digitally but applied as analog multiplications of RF-signals will in this chapter be denoted Analog Beamforming (ABF) adaptive antennas. The antenna signals are sampled and digitized by A/D-converters. This can be done in numerous ways (see [32]), e.g. after down conversion to the baseband or by narrowband sampling techniques at RF. The weighting of the RF-signals is done in hardware. The hardware weights can be implemented in various ways (see [28]), e.g. by software controlled attenuators and phase shifters. The weighting at RF will introduce a more complicated expression for the output SINR than the ideal expression given in (5.16). This is caused by two factors:

1) the weights are calculated based on quantized signals but are applied to non-quantized RF-signals, and

2) the analog weights are quantized.

Figure 5.4 shows a block diagram of an ABF adaptive antenna with the associated quantizations and also an equivalent noise model.
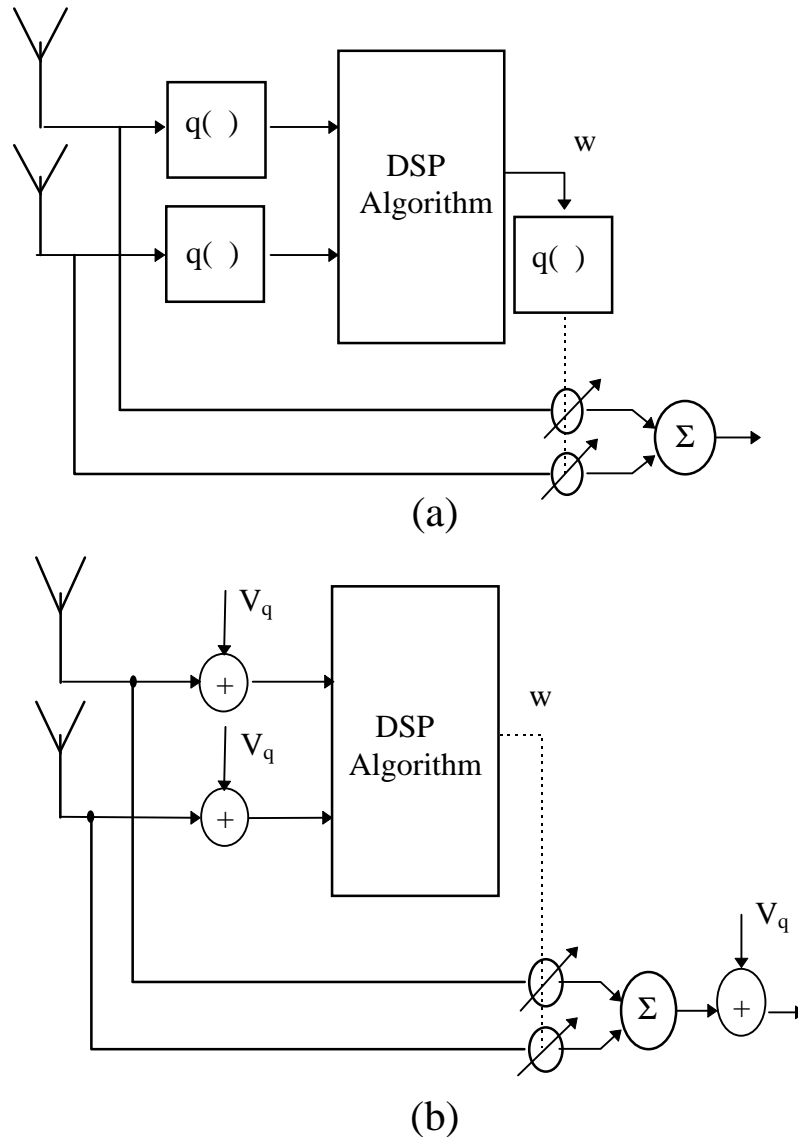
Fig. 5.4. Quantization block diagram (a) and equivalent noise model (b).
The operator q() represents quantization.

Consider first the implications of 1). We shall here extend the derivations
of [20] to the case were the noise vector used to calculate the weights
differ from the noise vector at the analog beamformer. This will be the
case since the hardware channels are different in the two cases, and also
because the calculations of the weights involve a signal quantization, see
Figure 5.9. The quantization noise can be considered uncorrelated if the
number of bits of the A/D converters are sufficiently large, see [33]. Let
σ_1^2 denote the average noise power (thermal noise and quantization noise)
of the signal used to calculate the weights, and σ_2^2 the average noise power
(only thermal noise) at the analog beamformer. This problem formulation
will not change the expressions in [20] for the desired and interfering
output power (other than that the noise per channel σ_1^2 now also contains

quantization noise) , but will give a new expression, compared to [20], for the output noise power. This expression is given by

$$P_n = \frac{\sigma_2^2}{\sigma_1^2} \frac{A_d^2 R^2 A_i^2}{2} \left(\frac{1}{\sigma_1^2 + \gamma}\right)^2 \left[\frac{\gamma \xi_i^{-1}}{A_d^2} - \left|\mathbf{u}_i^T \mathbf{u}_d^*\right|^2 \left(\frac{\xi_i^{-1}}{\xi_i^{-1} + \mathbf{u}_i^T \mathbf{u}_i^*}\right)^2\right]$$

(5.26)

where γ is given by

$$\gamma = A_d^2 \left[\mathbf{u}_d^T \mathbf{u}_d^* - \frac{\left|\mathbf{u}_d^T \mathbf{u}_i^*\right|^2}{\xi_i^{-1} + \mathbf{u}_i^T \mathbf{u}_i^*}\right]$$

(5.27)

The SINR of the adaptive antenna can therefore be written as

$$SINR = \frac{P_d}{P_i + P_n} = \frac{\gamma^2}{A_i^2 \left[\frac{\sigma_2^2}{\sigma_1^2} \gamma \xi_i^{-1} + A_d^2 \left(1 - \frac{\sigma_2^2}{\sigma_1^2}\right) \left(\frac{\xi_i^{-1}}{\xi_i^{-1} + \mathbf{u}_i^T \mathbf{u}_i^*}\right)^2 \left|\mathbf{u}_i^T \mathbf{u}_d^*\right|^2\right]}$$

(5.28)

$$\xi_d = \frac{A_d^2}{\sigma_1^2}$$

$$\xi_i = \frac{A_i^2}{\sigma_1^2}$$

Equation (5.28) constitutes a more complicated expression than the corresponding expression (5.16) for the ideal case. However, if the spatial correlation $|\mathbf{u}_d^T \mathbf{u}_i^*|$ between the desired and interfering signal is small, corresponding to a scenario where the interfering signal is well outside the main lobe of the adaptive antenna, the expression (5.28) reduces to

$$SINR \approx \frac{A_d^2 \mathbf{u}_d^T \mathbf{u}_d^*}{\sigma_2^2}$$

(5.29)

In this case, the SINR is approximately given by the ratio between the optimum combined desired signal and the *thermal noise* power per antenna channel. Note that the quantization noise power in this case does not affect the SINR since (5.29) does not depend on σ_1^2.

We have not yet considered the quantization of the analog weights when beamforming at RF. It can be shown that this will introduce a new noise term in the expression for the SINR proportional to the signal powers of the desired and interfering signals. This is the topic of the next section.

5.4.1 Weight Quantization

Quantization of the analog weights in both phase and amplitude will result in the following expression for the output power of the analog beamformer:

$$
\begin{aligned}
P &= E\left\{(\mathbf{w} + \Delta)^H \mathbf{x}\mathbf{x}^H (\mathbf{w} + \Delta)\right\} \\
&= E\left\{\mathbf{w}^H \mathbf{x}\mathbf{x}^H \mathbf{w}\right\} + 2 \cdot \mathrm{Re}\left(E\left\{\mathbf{w}^H \mathbf{x}\mathbf{x}^H \Delta\right\}\right) + E\left\{\Delta^H \mathbf{x}\mathbf{x}^H \Delta\right\}
\end{aligned}
\tag{5.30}
$$

where $\mathbf{w}$ is the ideal weight vector calculated by the processing unit, $\mathbf{x}$ the input vector at the array and Δ the complex error vector introduced by the quantization of the weight vector. Under the assumption that the error of the weight vector is uncorrelated with the weight vector itself the two terms in the middle of the expression can be neglected leaving

$$
P = E\left\{\mathbf{w}^H \mathbf{x}\mathbf{x}^H \mathbf{w}\right\} + E\left\{\Delta^H \mathbf{x}\mathbf{x}^H \Delta\right\}
\tag{5.31}
$$

The first term represents the ideal output power of the analog beamformer. The second term is the additional noise power originating from the weight quantization. Straightforward algebra reveals that the additional noise term can be expressed as

$$
E\left\{\Delta^H \mathbf{x}\mathbf{x}^H \Delta\right\} = E\left\{\left|\Delta_0\right|^2\right\} tr\{\Phi\}
\tag{5.32}
$$

provided that the variance of each component of the quantization error vector Δ is the same, namely $E\left\{\left|\Delta_0\right|^2\right\}$. The elements of the error *vector* Δ must be mutually independent, as well as Δ_i and x_i, for $i=1,2,\ldots,N$. The quantity $tr\{\Phi\}$ denotes the trace of the covariance matrix Φ, given by

$$tr\{\Phi\} = N \cdot \left\{A_d^2 + A_i^2 + \sigma_2^2\right\} \tag{5.33}$$

where A_d and A_i are the input magnitudes of the desired and interfering signals, σ_2^2 is the thermal noise at the beamformer output and N is the number of antenna elements. The final expression for the weight quantization noise will therefore be

$$E\left\{\Delta^H \mathbf{x}\mathbf{x}^H \Delta\right\} = E\left\{\left|\Delta_0\right|^2\right\} N\left\{A_d^2 + A_i^2 + \sigma_2^2\right\} \tag{5.34}$$

It is now straightforward to state a new expression for the output SINR of the analog beamformer. The expressions in [20] for the desired and interfering signal power will not be altered. The weight quantization noise power will however add to the original noise power of (5.26). The following expression is obtained:

$$SINR = \frac{R^2}{2}\left(\frac{\gamma}{\sigma^2 + \gamma}\right)^2 \Bigg/ \Bigg[\frac{A_i^2 R^2}{2}\left(\frac{1}{\sigma_1^2 + \gamma}\right)^2 \left\{\frac{\sigma_n^2}{\sigma_1^2}\gamma\xi_i^{-1} + \right.$$

$$+ A_d^2\left(1 - \frac{\sigma_2^2}{\sigma_1^2}\right)\left(\frac{\xi_i^{-1}}{\xi_i^{-1} + \mathbf{u}_i^T \mathbf{u}_i^*}\right)^2 \left|\mathbf{u}_i^T \mathbf{u}_d^*\right|^2 \Bigg\} + \tag{5.35}$$

$$+ E\left\{\left|\Delta_0\right|^2\right\} N\left\{A_d^2 + A_i^2 + \sigma_2^2\right\} \Bigg]$$

By again making the assumption that the *spatial correlation is low* ($\left|\mathbf{u}_d^T \mathbf{u}_i^*\right| \approx 0$), and also that the *desired signal power on the output is larger than the noise per antenna channel on the input* ($\gamma >> \sigma^2$), the expression (5.35) finally simplifies to

$$SINR \approx \frac{A_d^2 \mathbf{u}_d^T \mathbf{u}_d^*}{\sigma_2^2 + \frac{2}{R^2} E\left\{\left|\Delta_0\right|^2\right\} N\left\{A_d^2 + A_i^2 + \sigma_2^2\right\} A_d^2 \mathbf{u}_d^T \mathbf{u}_d^*}$$

(5.36)

where R is the magnitude of the reference signal. So, once again the adaptive antenna is able to suppress the interfering signal down below the noise floor, at the same time enhancing the desired signal. The noise floor in this case is however composed of two components; the thermal noise per channel and also a scaled version of the weight quantization noise. This noise floor will increase with increasing signal power ($A_d^2/2$ and $A_i^2/2$) at the input of the array. In particular, a strong desired signal will increase the noise floor. We can therefore conclude this section by stating that *the presence of quantization errors in the weights will reduce the SINR at the output of the array, especially for strong desired signals.* Equation (5.36) is further discussed and illustrated in Section 5.6.

5.5 Digital Beamforming

Ideally an adaptive antenna is able to suppress the interfering signal down to the noise floor, and at the same time enhancing the desired signal by optimum combining. Many components in the practical implementation of the adaptive antenna are involved in setting the overall noise level. The beamforming, i.e. application of the calculated adaptive antenna weights to the antenna signals, can be done either in software (digital beamforming, DBF) or in hardware (analog beamforming, ABF), described in the previous section. In the digital beamformer, the antenna signal is down-converted to a IF (intermediate frequency) or to the baseband before A/D conversion, see Figure 5.5. This arrangement gives a significant increase in weight accuracy compared to the ABF, but increases the system complexity, due to dynamic range considerations and high data rate support [34]. The A/D converter must be able to resolve a very weak signal, almost buried in noise, possibly in the presence of a strong signal from a mobile near the basestation. This put high demands on the A/D converters spurious free dynamic range (SFDR).
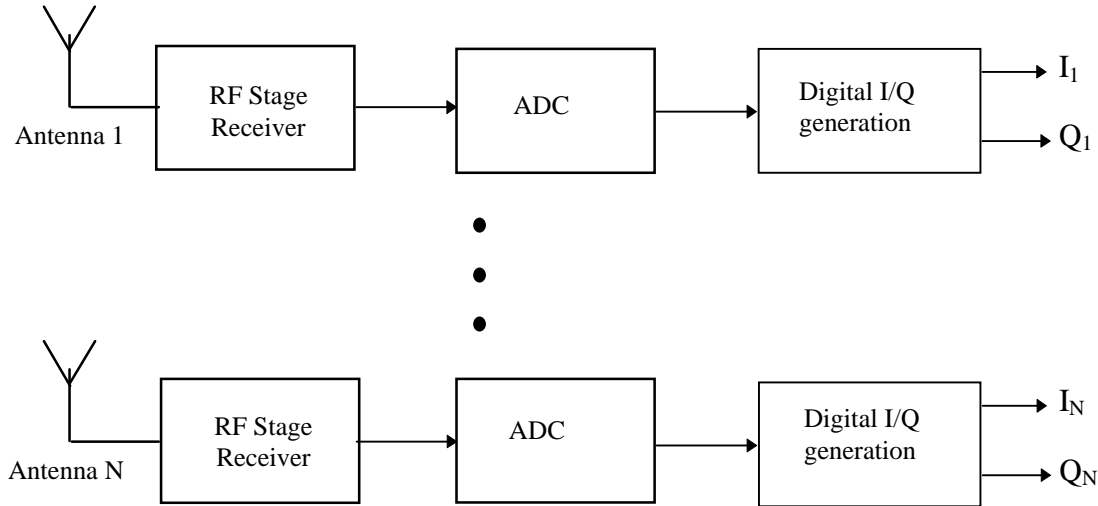
Fig. 5.5. Receiver using digital beamforming

Although (5.25) is valid for the DBF case as well, the errors in the weights when using the DBF is negligible in comparison with the previously described ABF due to the accuracy in the Digital Signal Processor (DSP). Assuming that the quantization noise variance σ^2_q is negligible compared to the thermal noise σ^2_n one notices that Equation (5.28) reduces to Equation (5.16), which is the SINR for an ideal array. The main error source in a DBF is thus not quantization error, but harmonic and intermodulation distortion introduced by the analog parts, such as amplifiers and the downconverting mixers. Thus, the key specifications of the digital beamformer is the spurious free dynamic range and the level of intermodulation distortion [35].

5.6 Calculation Example

In this section we will apply Equation (5.36) to the signal environment and antenna configuration presented in Table 5.1. We will show how the signal-power-dependent noise floor affects the improvement in SINR. Some minor approximations are made in order to simplify the derivations.

TABLE 5.1
EXAMPLE SCENARIO

Item	Specification
Signal environment	
Angle of desired signal	-61°
Angle of interfering signal	-7.2°
Thermal noise per channel	-72 dBm
Antenna configuration	
Array	Eight element Uniform Linear Array
A/D converter resolution	8 bits
Dynamic range A/D converter	48 dB
Weight resolution:	
phase	1 degree
magnitude	1 dB
Weight span	
phase	[0°, 360°]
magnitude	[0 dB, -50 dB]

$$\varepsilon_\theta = \frac{1}{2} \cdot \frac{\pi}{180}$$

$$\varepsilon_A 10^{a/20} = \frac{10^{(a+\Delta a)/20} - 10^{a/20}}{2}$$
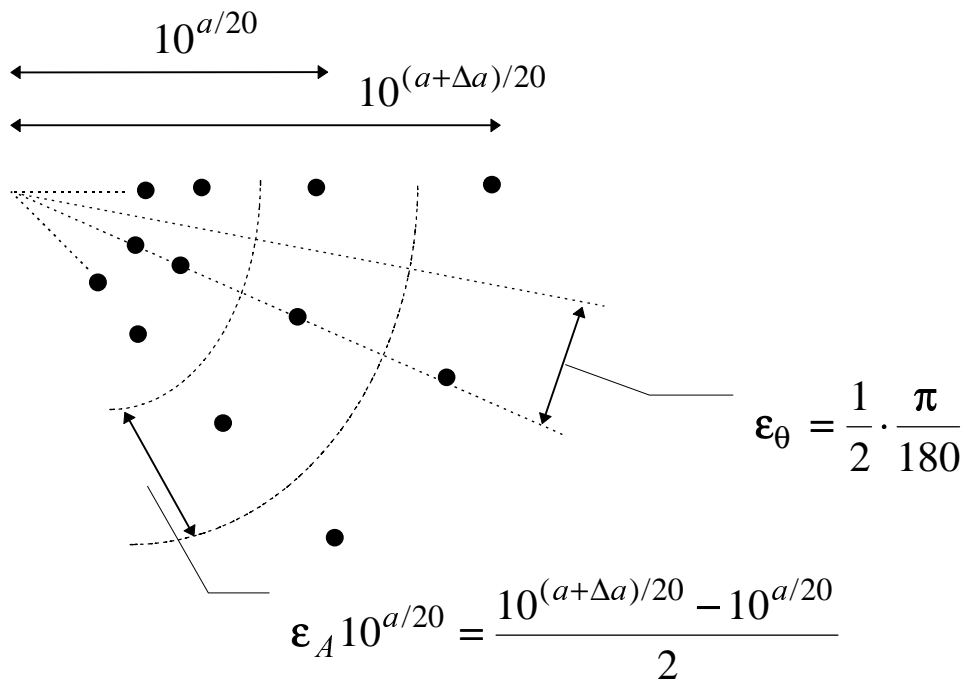
Fig. 5.6. Approximate quantization errors in amplitude and phase.

Equation (5.25) gives an expression for the variance of the weight magnitude quantization error utilizing the weight type considered here. A study of Figure 5.6 give approximate expressions for the relative error in magnitude and absolute error in phase, i.e.

$$\varepsilon_A = \frac{10^{(a+\Delta a)/20} - 10^{a/20}}{2 \cdot 10^{a/20}}$$ (5.37)

$$\varepsilon_\theta = 0.5\pi / 180$$

By assuming all weights to be of maximum magnitude we get the worst case expression for the variance of a single weight magnitude as

$$E\left\{|\Delta|^2\right\} \leq \frac{1}{3} \cdot 1^2 \cdot \left[\left(\frac{e^{1/20} - 1}{2}\right)^2 + \left(\frac{0.5\pi}{180}\right)^2\right] \approx 0.00024$$ (5.38)

An interesting figure of merit for the example antenna is the improvement of SINR, i.e. the ratio between the output SINR of the analog beamformer and the input SINR of an element channel. The SINR of an element channel is given by

$$SINR_{in} = \frac{A_d^2/2}{A_i^2/2 + \sigma_2^2}$$ (5.39)

and the approximate beamformer SINR by Equation (5.36), i.e.

$$SINR_{out} \approx \frac{A_d^2 \mathbf{u}_d^T \mathbf{u}_d^*}{P_r}$$ (5.40)

where P_r is given by

$$P_r = \sigma_2^2 + \frac{2}{R^2} E\left\{|\Delta_0|^2\right\} N\left\{A_d^2 + A_i^2 + \sigma_2^2\right\} A_d^2 \mathbf{u}_d^T \mathbf{u}_d^*.$$ (5.41)

The power P_r can in analogy with (5.29) and (5.36) be interpreted as the equivalent noise power per antenna channel of an ideal adaptive antenna. This gives the improvement as

$$\Delta(SINR) = \frac{SINR_{out}}{SINR_{in}} \approx \mathbf{u}_d^T \mathbf{u}_d^* \cdot \frac{A_i^2/2 + \sigma_2^2}{P_r} \cdot 2.$$ (5.42)

Equation (5.42) has two factors, the first containing the optimum gain of the array and the second the ratio between the interfering signal power plus thermal noise and the fictitious noise floor P_r. Since the optimum gain is independent of the signal power, the second factor will completely determine the behavior of $\Delta(SINR)$. The second factor illustrates that the interfering signal is suppressed down to P_r. By studying the signal-power-dependent P_r it is therefore easy to visualize the behavior of the adaptive antenna for different power levels of the desired and interfering signal. Calculated P_r and $\Delta(SINR)$ are depicted in Figure 5.7 (a) and (b), respectively.

(a)

(b)
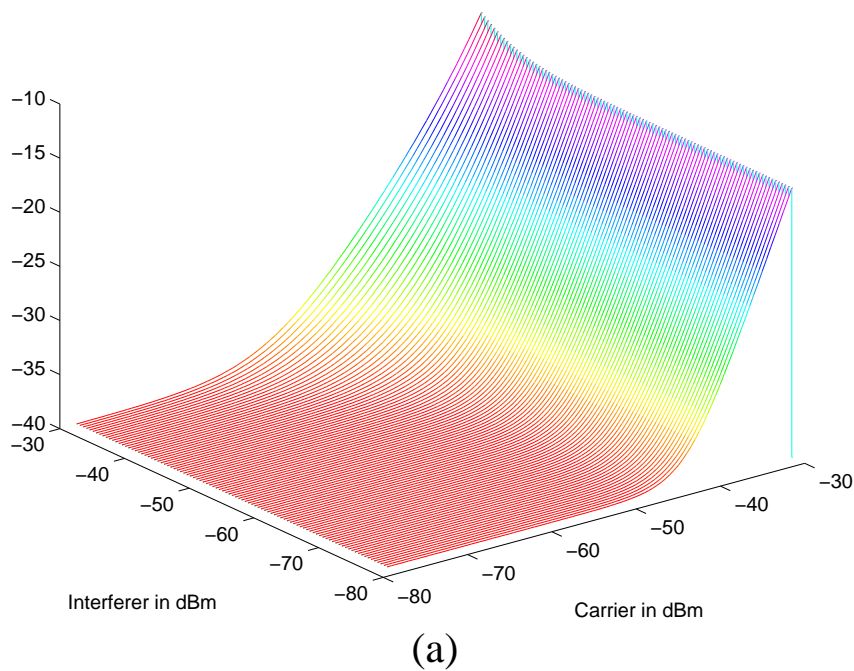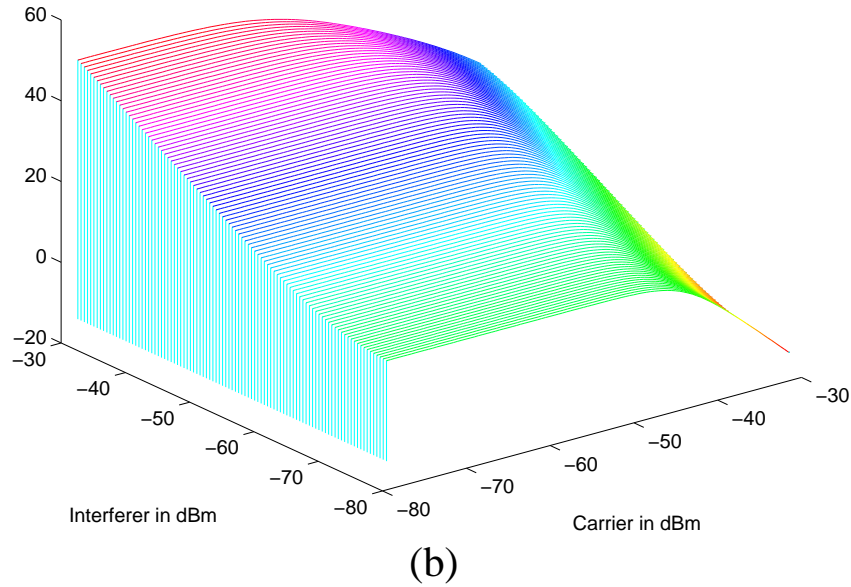
Fig. 5.7. Calculated fictitious noise floor P_r in dBm as a function of $A_d^2/2$ and $A_i^2/2$ (a), and SINR improvement in dB as a function of $A_d^2/2$ and $A_i^2/2$ (b).

Study for example P_r in Figure 5.7(a) along the line $A_d^2/2$=-75 dBm. Here the first term of (5.41) is dominant for all $A_i^2/2$, in other words P_r is constant for all interferer magnitudes. Now study Figure 5.7(b) along the same line. For $A_i^2/2$ below σ_2^2 we get a negligible increase in $\Delta(SINR)$ when plotted on a logarithmic scale, see (5.42). As $A_i^2/2$ exceeds σ_2^2 the interfering signal is suppressed down below P_r resulting in a linear increase in $\Delta(SINR)$. Along the line $A_d^2/2$=-50 dBm the first term of (5.41) is dominant for small values of $A_i^2/2$. As $A_i^2/2$ increases the third term dominates, resulting in an increase in P_r. For small values of $A_i^2/2$, $\Delta(SINR)$ will behave in the same manner as before. As P_r starts to increase we see a decreased increase in $\Delta(SINR)$. Along the line $A_d^2/2$=-35 dBm we actually get a negative $\Delta(SINR)$ for small values of $A_i^2/2$. This is due to the extremely high P_r caused by the second term of (5.41).

It is also interesting to study P_r along constant $A_i^2/2$-lines. Take for example $A_i^2/2$=-75 dBm, where for small values of $A_d^2/2$ the first term of (5.41) is dominant. As $A_d^2/2$ increases the second term of (5.41)

dominates, resulting in a linear increase in P_r. The slope of the increasing curve is two when plotted on a logarithmic scale because of the squared desired signal power. This will have an enormous impact on the $\Delta(SINR)$. Along the line $A_i^2/2$=-35 dBm we again have a constant P_r level for small values of $A_d^2/2$. P_r will then increase with increasing $A_d^2/2$ as the third term of (5.41) becomes the dominant one, resulting in a linear increase (slope one) in P_r for larger values of $A_d^2/2$. The decrease in $\Delta(SINR)$ is therefore not as dramatic as before.

Figure 5.8 shows the $\Delta(SINR)$ plotted in a different way, perhaps giving a better overview of the behavior of the adaptive antenna. For weak interference we see a constant level of improvement of the SINR. This is because the interference is well below the thermal noise, leaving only the optimum gain of the desired signal. As the interference power increases we get a linear increase in the SINR corresponding to the suppression of the interfering signal down below the fictitious noise floor. As the desired signal gets stronger the $\Delta(SINR)$ is decreasing resulting in a "bend" of the iso-lines (lines of equal $\Delta(SINR)$). For weak interference and a strong desired signal the SINR is actually impaired because of the enormous fictitious noise floor.
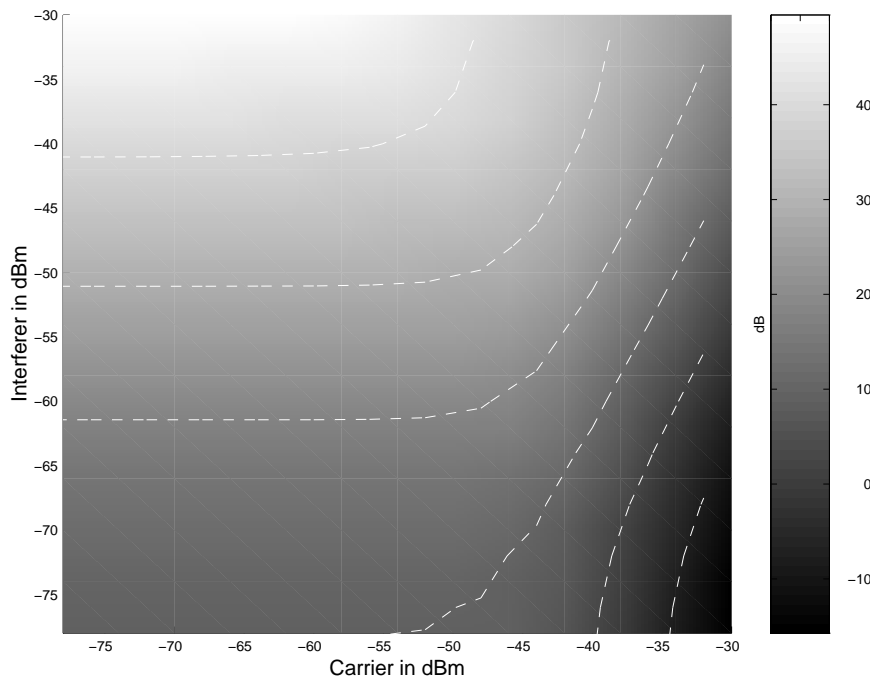
Fig. 5.8. Calculated SINR improvement in dB. The improvement decreases as the nuance of grey becomes more black.

5.7 Results

In this section the adaptive antenna system used to verify the theoretical results above is described, followed by a presentation of the measurement results.

5.7.1 Adaptive Antenna System

The adaptive antenna system operates partly according to DCS-1800 standards. However, only the uplink is implemented and only Traffic Channel (TCH) frames are transmitted for evaluation purposes. In each DCS-1800 time slot there is a 26 bit training sequence that is used as a reference signal in the signal processors for each of the two possible users on the same frequency and timeslot. The users are assigned different training signals, thus a multiple access scheme using SDMA is possible. The system is shown in Figure 5.9.
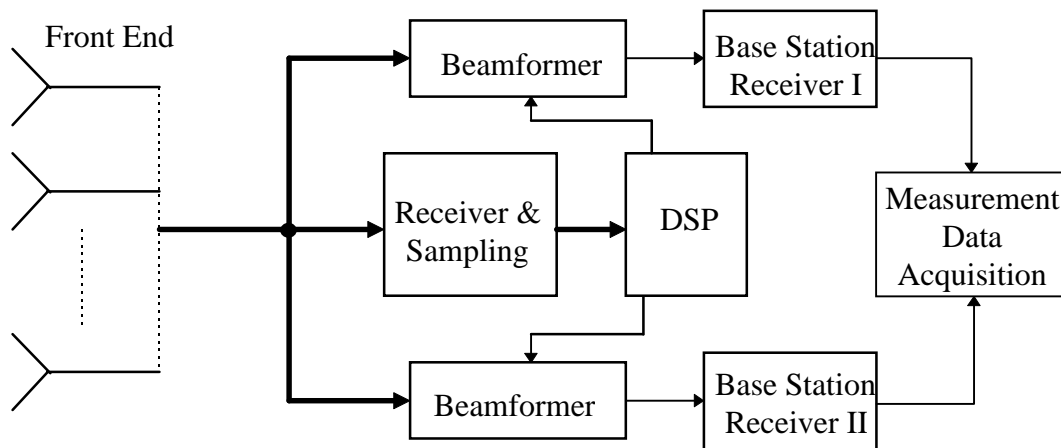
Fig. 5.9. Adaptive antenna system.

The front end consists of linearly polarized microstrip patch antenna elements with 80° beamwidth. The array is flexible and can be arranged in a linear or circular configuration with arbitrary element spacing. Up to ten antennas can be used in the array. The antenna signals are distributed to receivers and to two beamformers, which consists of phase shifters and signal attenuators that are digitally controlled by the DSP. The weighted signals are passively combined. Note that the weighting is performed at RF (radio frequency). The receivers down converts the signals to the baseband before sampling. Weight calculation is done by the DSP based on the

sampled signals. The weighted and summed RF signals are connected to ordinary base station receivers enabling measurements of BER, Frame Error Rate (FER) and other parameters characterizing the beamforming quality. For laboratory measurement purposes the antenna array is replaced by a Butler matrix that is fed by signal generators, giving rise to a scenario corresponding to two plane waves impinging on an eight element uniform linear array. Thus the adaptive antenna functionality can be verified without introducing difficulties of multipath propagation and fading.

5.7.2 Measurements of SINR

This section presents how the measurement of the improvement in SINR is performed. The measured quantity is not exact but is at least a good approximation of the true improvement in SINR, except when the CIR per antenna channel is high.

When measuring the improvement in SINR, first the signal levels of the desired signal and the interference are set. The adaptive antenna weights are then calculated and frozen. The interference is then removed and the output power of the analog beamformer measured. The measured power can then be expressed as

$$
\begin{aligned}
P_1 &= P_d + P_n + E\left\{\Delta^H (\mathbf{x}_d + \mathbf{x}_n)(\mathbf{x}_d + \mathbf{x}_n)^H \Delta\right\} = \\
&= P_d + P_n + N \cdot E\left\{|\Delta_0|^2\right\}\left(A_d^2 + \sigma_2^2\right)
\end{aligned}
\tag{5.43}
$$

where P_d is the desired signal output power given by (5.15) and P_n the output thermal noise power given by (5.26). The third term is the quantization noise power derived in Subsection 5.4.1. Note that the lack of the interfering signal in the power measurement only effects the third term, since the weights were calculated based on a signal environment containing both the desired signal and the interference.

The interfering signal source is then turned on, the desired signal removed, and once again the output power of the beamformer measured. The measured power in this case can be expressed as

$$P_2 = P_i + P_n + E\left\{\Delta^H (\mathbf{x}_i + \mathbf{x}_n)(\mathbf{x}_i + \mathbf{x}_n)^H \Delta\right\} =$$

$$= P_i + P_n + N \cdot E\left\{\left|\Delta_0\right|^2\right\}\left(A_i^2 + \sigma_2^2\right)$$

(5.44)

where P_i is the interference power given by (5.15). Now study the ratio of P_1 to P_2, i.e.

$$\frac{P_1}{P_2} = \frac{P_d}{P_i + P_n + N \cdot E\left\{\left|\Delta_0\right|^2\right\}\left(A_i^2 + \sigma_2^2\right)} +$$

$$+ \frac{P_n + N \cdot E\left\{\left|\Delta_0\right|^2\right\}\left(A_d^2 + \sigma_2^2\right)}{P_i + P_n + N \cdot E\left\{\left|\Delta_0\right|^2\right\}\left(A_i^2 + \sigma_2^2\right)}$$

(5.45)

It is most likely that the desired signal power of the beamformer output is greater than the output thermal noise plus quantization noise. The removal of the second term in Equation (5.45) is therefore not a very crude approximation, leaving

$$\frac{P_1}{P_2} \approx \frac{P_d}{P_i + P_n + N \cdot E\left\{\left|\Delta_0\right|^2\right\}\left(A_i^2 + \sigma_2^2\right)} \approx SINR_{out}$$

(5.46)

Equation (5.46) almost coincides with the exact expression for the output SINR of the ABF (see (5.36)). The difference is the lack of the term A_d^2 in the last parenthesis of the denominator. For interfering signals stronger than the desired signal at the input of the array, Equation (5.46) will therefore be a good approximation of the output SINR.

The input desired signal power and interference power is measured in turn at the input of the receivers (or input of the analog beamformer). In both measurements the signals are corrupted by the thermal noise of the antenna channel. The ratio of the two measurements can therefore be expressed as

$$\frac{A_d^2/2 + \sigma_2^2}{A_i^2/2 + \sigma_2^2} \approx \frac{A_d^2/2}{A_i^2/2 + \sigma_2^2} = SINR_{in}$$

(5.47)

The approximation in Equation (5.47) is valid for desired signals stronger than the thermal noise. The ratio between the measurements (approximately (5.46) and (5.47)) will therefore be a good approximation of the improvement of the SINR for the adaptive antenna, provided that the requirements above, made on signal levels and noise levels, are followed.

The practical measurements where made using two Gaussian Minimum Shift Keying (GMSK)-modulated signal sources connected to the inputs TR1 and TR4 of the Butler matrix, corresponding to a scenario of one signal source in direction -61° (azimuth plane) relative to broadside of a uniform linear array, and the other in direction -7.2°. The Sample Matrix Inversion (SMI) algorithm [36] was chosen for the calculation of the adaptive weights. (This method is also described in Chapter 4.) The measured improvement in SINR (calculated as the mean of nine measurements) is shown in Figure 5.10 (a) and (b), corresponding to beamformer one and two, respectively. These diagrams should be compared to Figure 5.8. The diagrams have much in common. Study the constant improvement for weak interference, the linear increase when the interference is increased and the decrease for increasing desired signal power, resulting in the "bend" of the iso-lines. Note however the rapid decrease of the measured improvement as the A/D converters saturate for strong desired signals (>-40 dBm). It can also be seen that the measured and calculated improvement of the SINR differ for desired signals much stronger than the interferer, see Figure 5.8. This is not surprising since the approximations we have made above are not valid in this region.

(a)

(b)
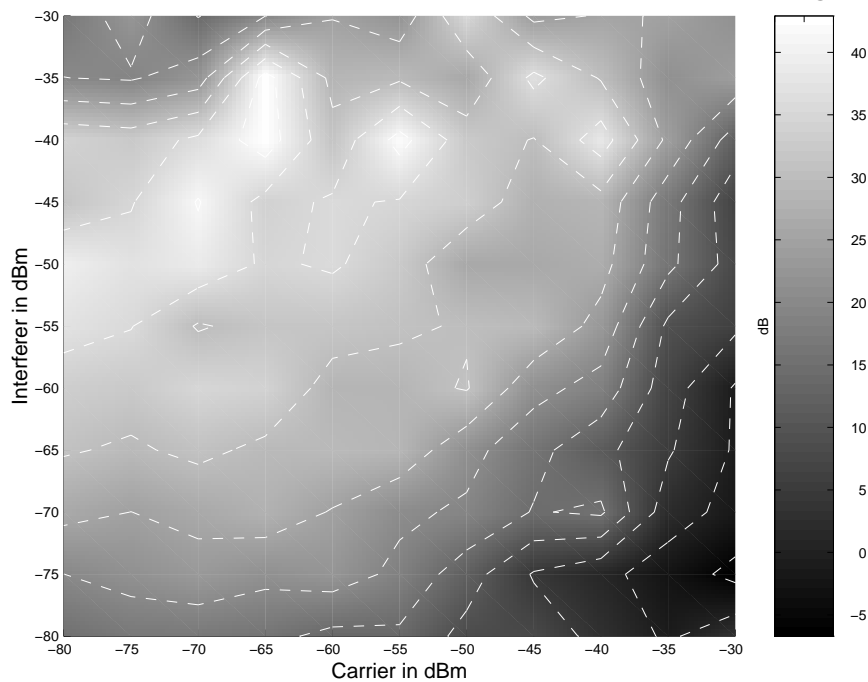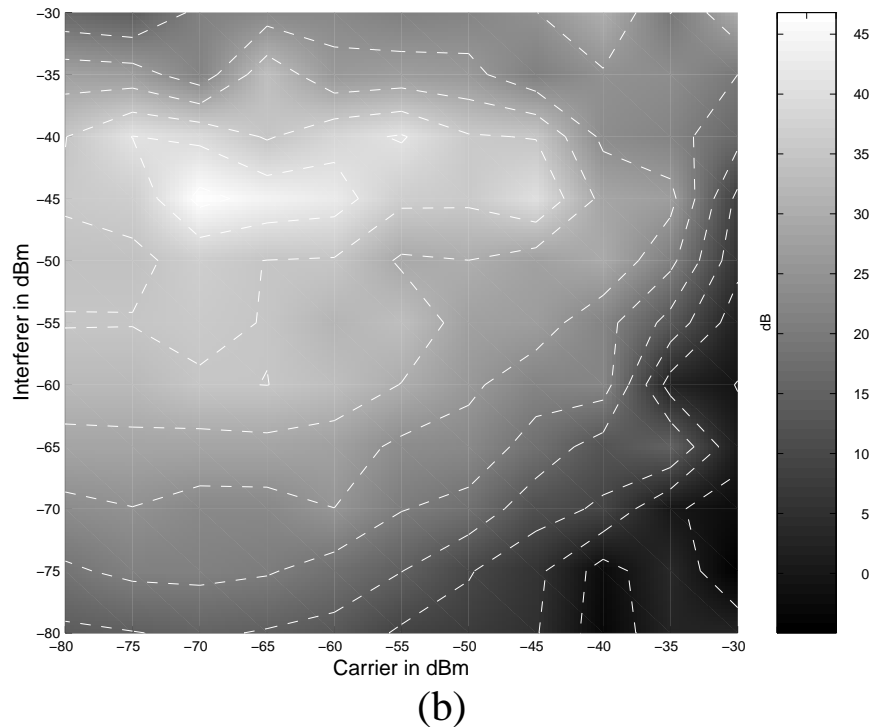
Fig. 5.10 Measured SINR improvement in dB for beamformer 1 (a) and beamformer 2 (b). The improvement decreases as the nuance of grey becomes more black. Note the overestimation of the improvement for strong carriers and weak interference compared to Figure 5.11. This is because the measurement is not valid in that region.

5.7.3 Field Trial Measurements

The measurements described in the previous section were conducted in a laboratory using a Butler matrix as a substitute for the array antenna. Those measurements gave information about the adaptive antenna performance in an ideal environment, with omnidirectional radiation patterns with equal gain. The next step in the evaluation process is to perform measurements using the real front end with directive antenna element patterns placed in a circular array configuration. The measurements were made on an outdoor antenna measurement site with no reflective buildings or other objects in the surroundings. The front end was placed on a turntable tower. This gave possibilities to measure static antenna diagrams, which provide insight into how adaptive antennas work. The measurements are static and yield no information of the dynamic performance of the antenna when signal sources are moving. Measurements of the improvement in signal to interference plus noise ratio with different separations of signal sources were made and the results are presented below. The adaptive antenna performance severely degrades

when the angular separation is less than 20 degrees. This is due to the high spatial correlation between the signal sources as discussed in Subsection 5.2.2. As presented below, the measurements of the dynamic performance, although averaged, were made by moving the signal sources along an arc, while keeping the distance to the base station antenna constant, and simultaneously measuring the BER as a function of the angular separation. For more results from these field trials, see [37], [38] and Chapter 4.

5.7.4 Improvement of SINR at Different Angular Separations

The impact of spatial correlation is illustrated by measuring the SINR for different Direction of Arrival (DOA) separation of the desired and interfering signal, with the circular array field trial arrangement.
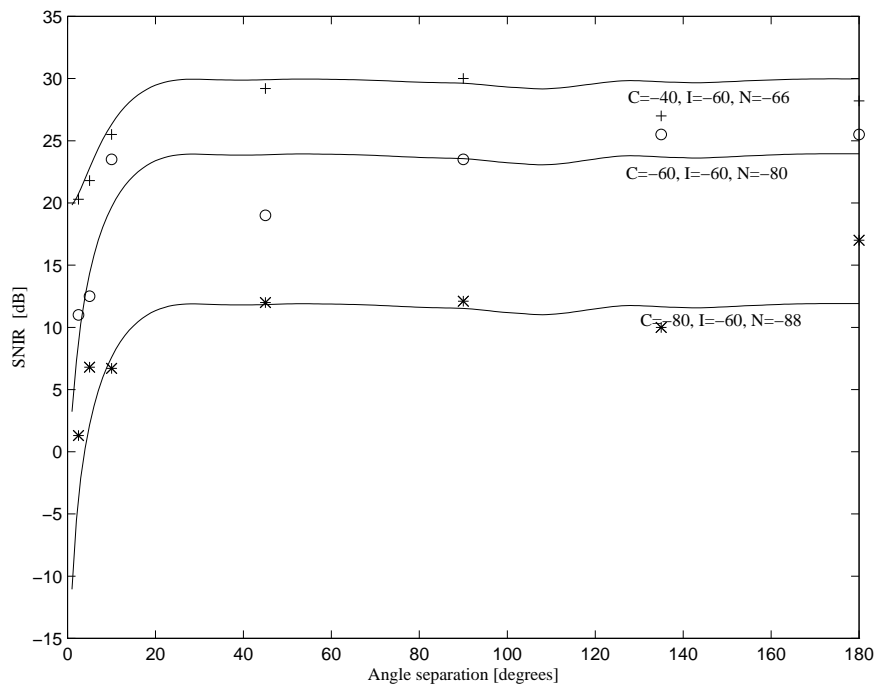
Fig. 5.11. SINR as a function of mobile separation, using measured element patterns. Solid is fitted theoretical, markers is measured data.

As seen in Figure 5.11, the adaptive array performance, measured in SINR of the adaptive antenna output, is degraded when the angle separation is decreased. The experimental results show a qualitative agreement with the theory developed in Subsection 5.2.2 (recall Equation (5.35)). However, the noise parameters are unmeasurable, so an approximate curve fit using Equation (5.16) is shown in Figure 5.11, to qualitatively show the impact of spatial correlation. The noise power is the variable fitting parameter. At separation angles above 20°, the SINR is approximately constant. The

SINR level is determined by the signal powers and noise power at the antenna input. When the angle is decreased below 20° the degree of spatial correlation between the two signal sources increases and this SINR degrades, in agreement with Equation (5.16). When the power of the carrier is increased, the increase in noise power is non-linear due to the weight quantization. So the rate of change in SINR is decreasing with increasing received power, see Figure 5.11. This observation verifies the discussion in Section 5.6 and Equation (5.35).

5.7.5 Using BER as a Performance Measure

In the previous parts of this chapter the adaptive antenna performance has been investigated in terms of improvement in SINR. The BER was also measured as a function of the separation in angle between the desired and interfering mobile when the two transmitters were moving towards (and past) each other. The power received from the two mobiles are varied to emulate the near-far effect. The BER is a function of the SINR at receiver input. When SINR is decreased below a certain threshold level, the BER is rapidly increased to about 50% and the communication link is lost. This problem must be solved in a future SDMA system by performing an intra-cell handover, i.e. one of the mobiles must change transmitting and receiving frequencies or time slots.

The SINR is dependent on the transmitting power of the desired and interfering mobiles and their spatial correlation, which approaches one when their angle approaches zero as seen in Subsection 5.2.2. In Figure 5.12 the BER as a function of separation between a desired and interfering mobile is presented for different settings of transmitted powers. The curves represents the class II bits (not protected by coding) in the DCS-1800 standards. The measurements are performed in the same environment as in Subsection 5.7.3.
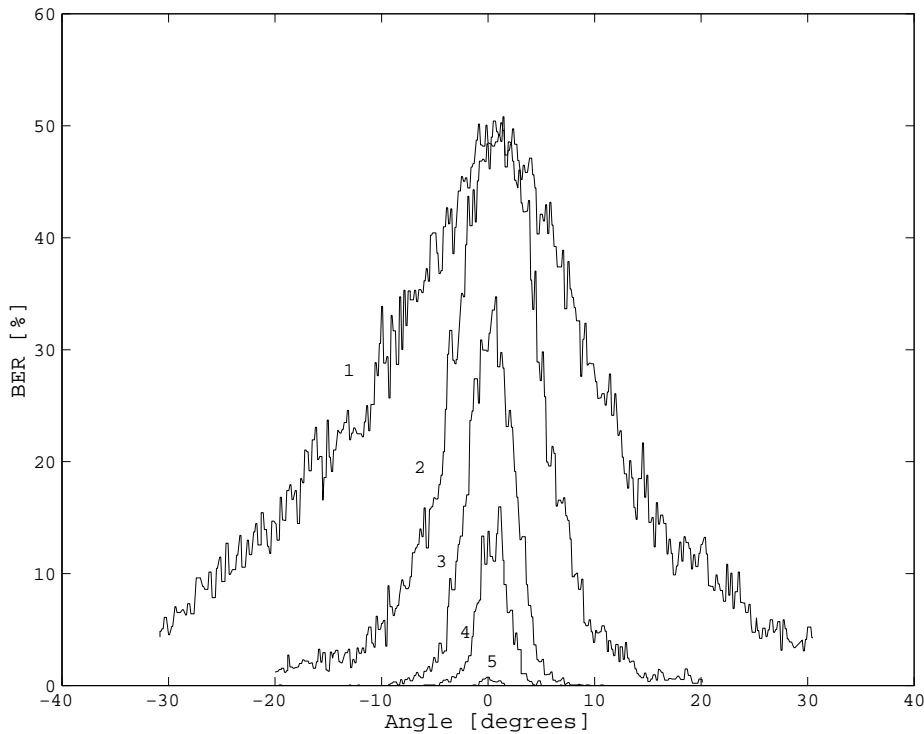
Fig. 5.12. BER as a function of interferer and desired signal DOA separation in horizontal plane. Unprotected (Class II) bits. SIR=-25 dB (1), -20 dB (2), -15 dB (3), -10 dB (4), 0 dB (5).

The behavior of the curves in Figure 5.12 can be explained by the spatial correlation measurement presented in Figure 5.11. The threshold level for the SINR giving a BER of approximately 0 % is about 9 dB in the DCS-1800 standard. When the separation angle is greater than 20 degrees the SINR is approximately constant at a level determined by the input of the desired and interfering signal powers. If the ratio of the input powers are greater than -20 dB, the antenna manages to suppress the interferer enough to give a BER close to 0 % as seen in Figure 5.12, curve 2-5. If the power ratio is below -25 dB, the improvement in SINR is not enough to provide an output SINR above 9 dB and the BER will therefore be well above 0 % for all angular separations, see curve 1 in Figure 5.12. When the angular separation is less than 20 degrees the high spatial correlation severely degrades the output SINR, as can be seen in Figure 5.11.